A new BEM for solving multi-medium transient heat conduction

***Wei-Zhe Feng[1], Kai Yang[1], Hai-Feng Peng[1], †Xiao-Wei Gao[1, 2]**

[1]School of Aeronautics and Astronautics, Dalian University of Technology,
Dalian 116024, P.R. China
[2]State Key Laboratory of Structural Analysis for Industrial Equipment,

*Presenting author: fengwz@mail.dlut.edu.cn
†Corresponding author: xwgao@dlut.edu.cn

Abstract

In this paper, a new single interface integral equation method is presented for solving transient heat conduction problems consisting of multi-medium materials with variable thermal properties. Firstly, adopting the fundamental solution for the Laplace equation, the boundary-domain integral equation for transient heat conduction in single medium is established. Then from the established integral equation, a new single interface integral equation is derived for transient heat conduction in general multi-medium functionally graded materials, by making use of the variation feature of the material properties. The derived formulation, which makes up for the lack of boundary integral equation in solving multi-medium problems, has the feature that only a single boundary integral equation is used to solve multi-medium transient heat conduction problems. Compared with conventional multi-domain boundary element method, the newly proposed method is more efficient in data preparing, program coding and computational cost. Based on the implicit backward differentiation scheme, an unconditionally stable and non-oscillatory time marching solution scheme is developed for solving the time-dependent system of differential equations. Numerical examples are given to verify the correctness of the presented method.

Keywords*:* Transient heat conduction, Multi-medium problems, Non-homogeneous problem, Interface integral equation.

1. Introduction

With the advantages of semi-analytical feature and dimensional reduction characteristic, the boundary element method (BEM) has been successfully applied to solve transient heat conduction problems [1-4]. According to the differences of solution procedures, most of the existing approaches can be classified into two broad categories: the transformed space approach (Rizzo and Shippy [5]; Sutradhar et al.[6]; Sutradhar and Paulino [7]; Simoes[8]; Guo et al. [9]), and the time domain approach (Wrobel and Brebbia [10]; Ochiai et al.[11]; Tanaka et al.[12]; Yang and Gao[13]; Al-Jawary el al. [14]; Yu et al. [15]). In the transformed space approach, the time dependent derivative is removed by applying an algebraic transform variable, and the system of equations is solved in the transform space, then inverse transform is employed to reconstitute the solution in time domain. The other kind is the time domain approach, by which the solutions are found directly in the time domain. One implementation of the time domain approach is the use of time-dependent fundamental solution [10, 11], that can result in a pure boundary integral equation algorithm. However, numerically evaluating the boundary integrals requires both space and time discretization. More details about time-dependent fundamental solution approaches can be found in the works of Wrobel and Brebbia [10] and Ochiai and Sladek [11]. Another implementation of the time domain approach is to employ the fundamental solution for the Laplace equation, and transform the volume integrals associated with time dependent derivative into equivalent boundary integrals. Among the transforming techniques, the dual reciprocity method (DRM) [16, 17], Multiple reciprocity method (MRM) [18], and radial integration method (RIM) [19] are most widely used.

Transient heat conduction BEM has been broadened to a wide range of engineering problems, including non-homogeneous [21], anisotropic [20], and non-linear problems [33]. But most studies mainly focus on single medium. However, most engineering problems involve objects composed of different materials. Therefore, it is important to develop the multi-medium BEM. The conventional widely used technique for solving multi-medium problems is the multi-domain boundary element method (MDBEM) [25-29]. The basic idea of this method is that the whole domain of concern is broken up into a number of separate sub-domains, then a boundary integral equation is written for each sub-domain, and the final system of equations is formed by assembling all contributions of the discretized integral equations for each sub-domain based on the compatibility condition and equilibrium relationship. In the transient heat conduction field, Erhart et al. [31] developed a parallel domain decomposition Laplace transform BEM algorithm for solving the large-scale transient heat conduction problems. Recently, Gao et al. [25, 32] proposed a three-step multi-domain BEM for solving multi-medium non-homogeneous problems.

Although MDBEM is flexible in solving multi-medium problems, it has disadvantages in data preparation and computational time, since twice the element information over the same interface needs to be defined for the adjacent two sub-domains, and twice integrations need to be carried out over interface elements. Moreover, the variable condensation and assembling processes require a higher coding skill to develop a universal program, which heavily influences the computational efficiency. Tracing the issue to its source, the existing boundary integral equations were established on a single medium assumption, therefore it is awkward to solve multi-medium problems through using MDBEM, which involves tedious domain decomposing and assembling processes.

Recently, Gao and his coworkers proposed a single integral equation method, named interface integral BEM (IIBEM), for solving multi-medium problems [34-37]. Through a degeneration method from domain to interface integrals, the integral equation for solving single medium problems can be extended to interface integral equation capable of solving multi-medium steady heat conduction [34], elasticity [35, 36] and elastoplasticity [37] problems. Comparing with the conventional boundary integral equation, an additional interface integral appears in the basic integral equation, embodying the difference of material properties between two adjacent media. The derived formulations make up for the lack of a boundary integral equation in solving multi-medium problems. Compared with MDBEM, the derived integral equation is very simple in form and only requires integration once over the interface elements. Attributed to the feature of being single integral equation, it is easy to adopt the fast multi-pole method to solve large-scale problems [41].

In this paper, a new single integral equation method is developed for solving general multi-medium transient heat conduction problems. Firstly, the boundary-domain integral equation for single medium non-homogeneous transient heat conduction is established. Then from the established integral equation, the interface integral equation for multi-medium transient heat conduction problems is derived, by a degeneration technique from a domain integral to an interface integral. The new formulation allows the thermal material properties (i.e., thermal conductivity, specific heat and mass density) varying spatially within each medium, and jump across the interfaces between every two adjacent different media. For the first time, a single integral equation method is employed to solve multi-medium transient heat conduction problems with variable material properties.

To solve the time-dependent system of differential equations, the finite difference method (FDM) is used in the discretization of time to approximate the time evolution of temperatures. Based on an implicit backward differentiation scheme, an unconditionally stable and non-oscillatory time marching solution scheme is developed for solving the normal time-dependent system of equations, in which only temperature is involved as the time-dependent unknown variable. Numerical examples are given to verify the correctness of the presented method. The results show that, the presented formulations are robust in solving transient heat conduction in multi-medium functionally graded materials.

2. Review of boundary-domain integral equation for transient heat conduction in single non-homogeneous medium

In this paper, the thermal conductivity *k*, specific heat c_p and mass density ρ are assumed to be functions of spatial coordinates $\mathbf{x}$, i.e. $k(\mathbf{x})$, $c_p(\mathbf{x})$, $\rho(\mathbf{x})$. In this case, the governing equation for transient heat conduction problems can be written as follows:

$$\nabla\left[k(\mathbf{x})\nabla T(\mathbf{x},t)\right]+Q(\mathbf{x})=\rho(\mathbf{x})c_p(\mathbf{x})\frac{\partial T(\mathbf{x},t)}{\partial t} \qquad (t>t_0,\ \mathbf{x}\in\Omega) \tag{1}$$

where, $T(\mathbf{x},t)$ is the temperature at location $\mathbf{x}$ at time *t*; $Q(\mathbf{x})$ is the heat generation; t_0 is the initial time, and Ω represents the computational domain.

The initial condition is

$$T(\mathbf{x},0)=T_0(\mathbf{x}) \tag{2}$$

where, $T_0(\mathbf{x})$ is the initial temperature. On the boundary, Dirichlet and Neumann boundary conditions are prescribed as follows:

$$T(\mathbf{x},t) = \overline{T}(\mathbf{x},t), \qquad \mathbf{x} \in \Gamma_T \tag{3}$$

$$q(\mathbf{x},t) = -k(\mathbf{x})\frac{\partial T(\mathbf{x},t)}{\partial n} = \overline{q}(\mathbf{x},t), \qquad \mathbf{x} \in \Gamma_q \tag{4}$$

where, $q(\mathbf{x},t)$ is the normal heat flux on the boundary Γ of the computational domain Ω; n is the unit outward normal to Γ; and $\Gamma = C(\Gamma_T \bigcup \Gamma_q) = \partial\Omega$, $\Gamma_T \bigcap \Gamma_q = \varnothing$. In Eqs. (3) and (4), $\overline{T}(\mathbf{x},t)$, $\overline{q}(\mathbf{x},t)$ are the given temperature and heat flux on the boundary, usually prescribed as given functions.

Taking the fundamental solution for the Laplace equation as the weight function, applying the weighted residual technique to Eq.(1), and using the Gauss' divergence theorem, the boundary-domain integral equation for solving single medium transient heat conduction problems can be established [13]:

$$\begin{aligned} c\tilde{T}(\mathbf{y},t) = & -\int_\Gamma G(\mathbf{x},\mathbf{y})\, q(\mathbf{x},t)\, d\,\Gamma(\mathbf{x}) - \int_\Gamma \frac{\partial G(\mathbf{x},\mathbf{y})}{\partial n} \tilde{T}(\mathbf{x},t)\, d\,\Gamma(\mathbf{x}) \\ & + \int_\Omega G(\mathbf{x},\mathbf{y})\, Q(\mathbf{x})\, d\,\Omega(\mathbf{x}) + \int_\Omega V(\mathbf{x},\mathbf{y})\, \tilde{T}(\mathbf{x},t)\, d\,\Omega(\mathbf{x}) \\ & - \int_\Omega \frac{\rho(\mathbf{x}) c_p(\mathbf{x})}{k(\mathbf{x})} G(\mathbf{x},\mathbf{y}) \frac{\partial \tilde{T}(\mathbf{x},t)}{\partial t}\, d\,\Omega(\mathbf{x}) \end{aligned} \tag{5}$$

where c =1 for internal points and 1/2 for smooth boundary points; $\mathbf{y}$ represents the source point, and $\mathbf{x}$ the field point; $G(\mathbf{x},\mathbf{y})$ is the fundamental solution for Laplace equation, $\partial G(\mathbf{x},\mathbf{y})/\partial n$ and $V(\mathbf{x},\mathbf{y})$ are the derived kernels. These quantities can be expressed as follows

$$G(\mathbf{x},\mathbf{y}) = \begin{cases} \dfrac{1}{2\pi}\ln(\dfrac{1}{r}) & \text{for 2D problem} \\ \dfrac{1}{4\pi r} & \text{for 3D problem} \end{cases} \tag{6}$$

$$\frac{\partial G(\mathbf{x},\mathbf{y})}{\partial n} = \frac{\partial G(\mathbf{x},\mathbf{y})}{\partial x_i} n_i(\mathbf{x}) = \frac{-1}{2\alpha\, r^\alpha} \frac{\partial r}{\partial x_i} n_i \tag{7}$$

$$\begin{aligned} V(\mathbf{x},\mathbf{y}) &= \frac{\partial G(\mathbf{x},\mathbf{y})}{\partial x_i} \frac{\partial \tilde{k}(\mathbf{x})}{\partial x_i} \\ &= \frac{\partial G(\mathbf{x},\mathbf{y})}{\partial x_i} \frac{1}{k(\mathbf{x})} \frac{\partial k(\mathbf{x})}{\partial x_i} \end{aligned} \tag{8}$$

where, $\alpha = \beta - 1$ ($\beta = 2$ for 2D problems and 3 for 3D problems); *r* is the distance between source point $\mathbf{y}$ and field point $\mathbf{x}$; $\partial r / \partial x_i$ is the partial derivative of *r* with respect to coordinate x_i; n_i is the *i*-th component of *n*. In Eqs. (7) and (8) and through the paper, the repeated subscripts represent summation.

In Eq. (5) normalized temperature and thermal conductivity are utilized, by considering the product of temperature and thermal conductivity as the unknown variable [13, 38]

$$\tilde{T}(\mathbf{x}) = k(\mathbf{x})T(\mathbf{x}) \tag{9}$$

$$\tilde{k}(\mathbf{x}) = \ln k(\mathbf{x}) \tag{10}$$

Integral equation (5) is the boundary-domain integral equation for solving general single medium transient heat conduction problems. And through the radial integration method (RIM) transforming the involved domain integrals in Eq.(5) to the boundary, a pure boundary element algorithm without internal cells for single medium transient heat conduction can be developed [13].

From Eq.(10) we can see that the kernel function $V(\mathbf{x},\mathbf{y})$ involves the spatial derivative of the thermal conductivity $\partial k(\mathbf{x})/\partial x_i$, which indicates that $k(\mathbf{x})$ should vary continuously without jump in the domain Ω. However, for a problem consisting of multiple media, the thermal conductivity jumps across the interfaces between two adjacent materials, the derivative $\partial k(\mathbf{x})/\partial x_i$ will lead to an infinity. Therefore, Eq.(5) is not valid for multi-medium problems. However, the singular kernel is in fact integrable as shown in section 3. In section 3, we will deal with multi-medium problems in which the conductivity is not continuous across the interfaces of media. In this case, the domain integral involved in Eq. (5) is degenerated into an interface integral between two adjacent materials.

3. Interface integral equation for multi-medium transient heat conduction

For the sake of convenience and not losing generality, a problem consisting of two media characterized by conductivities $k_1(\mathbf{x})$ and $k_2(\mathbf{x})$ is considered as shown in Fig. 1, in which Γ is the outer boundary of the problem, Γ_I is the interface between media $k_1(\mathbf{x})$ and $k_2(\mathbf{x})$, and n' is the outward normal to Γ_I. Since the thermal conductivity jumps across the interface Γ_I, we separate a narrow domain Ω_3 around Γ_I, which has a constant infinitesimal thickness Δh along the interface (see Fig.1).

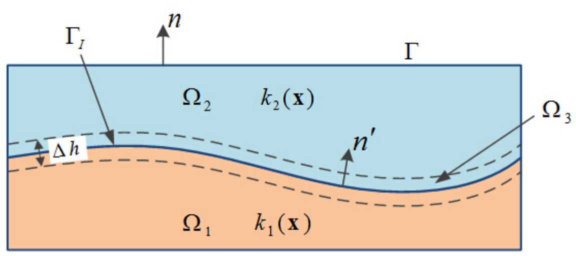

Figure 1. A narrow domain separated around interface of two media

Referring to Fig. 1, the domain integral involving kernel $V(\mathbf{x},\mathbf{y})$ in Eq. (4) can be written as

$$\begin{aligned}\int_{\Omega} V(\mathbf{x},\mathbf{y})\,\tilde{T}(\mathbf{x},t)d\Omega &= \lim_{\Delta h\to 0}\left(\int_{\Omega_1+\Omega_2} V(\mathbf{x},\mathbf{y})\,\tilde{T}(\mathbf{x},t)\,d\Omega\right)+\lim_{\Delta h\to 0}\left(\int_{\Omega_3} V(\mathbf{x},\mathbf{y})\,\tilde{T}(\mathbf{x},t)\,d\Omega\right)\\ &= \int_{\overline{\Omega}} V(\mathbf{x},\mathbf{y})\,\tilde{T}(\mathbf{x},t)\,d\Omega+\lim_{\Delta h\to 0}\left(\Delta h\int_{\Gamma_I} V(\mathbf{x},\mathbf{y})\,\tilde{T}(\mathbf{x},t)\,d\Gamma\right)\end{aligned} \tag{11}$$

where $\overline{\Omega}$ represents the whole integration domain consisting of all media with an infinite narrow domain isolated out, and in a specific medium $V(\mathbf{x},\mathbf{y})$ is determined by Eq.(8). From Eq.(8), we can see that the kernel $V(\mathbf{x},\mathbf{y})$ involved in the above equation is related to the gradient of the normalized conductivity $\partial\tilde{k}(\mathbf{x})/x_i$. With the existence of a jump effect across the interface Γ_I, the second integral item on the right hand side of Eq.(8) can be manipulated as follows [34, 37]:

$$\begin{aligned}\lim_{\Delta h\to 0}\left(\Delta h\int_{\Gamma_I} V(\mathbf{x},\mathbf{y})\,\tilde{T}(\mathbf{x},t)\,d\Gamma\right) &= \int_{\Gamma_I}\frac{\partial G(\mathbf{x},\mathbf{y})}{\partial x_i}\,n_i'\,\frac{1}{k(\mathbf{x})}\,\Delta k(\mathbf{x})\,\tilde{T}(\mathbf{x},t)\,d\Gamma\\ &= \int_{\Gamma_I}\frac{\partial G(x,y)}{\partial n_i'}\,\Delta k(\mathbf{x})\,T(\mathbf{x},t)\,d\Gamma\end{aligned} \tag{12}$$

Substituting Eq.(12) into Eq.(11), and the result into Eq.(5), the final temperature integral equation is derived as follows:

$$\begin{aligned} c\,\tilde{T}(\mathbf{y},t) &= -\int_{\Gamma} G(\mathbf{x},\mathbf{y})\,q(\mathbf{x},t)\,d\,\Gamma(\mathbf{x}) - \int_{\Gamma}\frac{\partial G(\mathbf{x},\mathbf{y})}{\partial n}\,\tilde{T}(\mathbf{x},t)\,d\,\Gamma(\mathbf{x})\\ &\quad+\int_{\Gamma_I}\frac{\partial G(\mathbf{x},\mathbf{y})}{\partial n'}\,\Delta k(\mathbf{x})\,T(\mathbf{x},t)\,d\,\Gamma(\mathbf{x})+\int_{\Omega} G(\mathbf{x},\mathbf{y})\,Q(\mathbf{x})\,d\,\Omega(\mathbf{x})\\ &\quad+\int_{\overline{\Omega}} V(\mathbf{x},\mathbf{y})\,\tilde{T}(\mathbf{x},t)\,d\,\Omega(\mathbf{x})-\int_{\Omega}\frac{\rho(\mathbf{x})c_p(\mathbf{x})}{k(\mathbf{x})}\,G(\mathbf{x},\mathbf{y})\,\frac{\partial\tilde{T}(\mathbf{x},t)}{\partial t}\,d\,\Omega(\mathbf{x})\end{aligned} \tag{13}$$

Eq.(13) is the established interface integral equation for solving multi-medium transient heat conduction problems. The time-dependent effect is embodied by the domain integral involving the time derivative of temperature $\partial\tilde{T}(\mathbf{x},t)/\partial t$. The jump effect of thermal conductivities across the interfaces between every two adjacent media is embodied by the interface integral item carried out on Γ_I; The non-homogeneous effect of material properties is embodied by the domain integral item involving kernel $V(\mathbf{x},\mathbf{y})$.

In numerical implementation, three types of points are introduced in discretization: outer boundary points on Γ, interface points on Γ_I, and internal points in Ω. Eq.(13) is only suitable for the outer boundary points and internal points by setting $c = 1/2$ for smooth outer boundary and $c = 1$ for internal points, respectively. When the source point $\mathbf{y}$ is located on the interface points, a similar integral equation can be obtained by letting $\mathbf{y} \to \Gamma_I$ [34]:

$$
\begin{aligned}
c^I\, \tilde{T}(\mathbf{y}^I, t) = & -\int_\Gamma G(\mathbf{x},\mathbf{y}^I)\, q(\mathbf{x},t)\, d\,\Gamma(\mathbf{x}) - \int_\Gamma \frac{\partial G(\mathbf{x},\mathbf{y}^I)}{\partial n} \tilde{T}(\mathbf{x},t)\, d\,\Gamma(\mathbf{x}) \\
& + \int_{\Gamma_I} \frac{\partial G(\mathbf{x},\mathbf{y}^I)}{\partial n'} \Delta k(\mathbf{x})\, T(\mathbf{x},t)\, d\,\Gamma(\mathbf{x}) + \int_\Omega G(\mathbf{x},\mathbf{y}^I)\, Q(\mathbf{x})\, d\,\Omega(\mathbf{x}) \\
& + \int_{\overline{\Omega}} V(\mathbf{x},\mathbf{y}^I)\, \tilde{T}(\mathbf{x},t)\, d\,\Omega(\mathbf{x}) - \int_\Omega \frac{\rho(\mathbf{x}) c_p(\mathbf{x})}{k(\mathbf{x})} G(\mathbf{x},\mathbf{y}^I) \frac{\partial \tilde{T}(\mathbf{x},t)}{\partial t}\, d\,\Omega(\mathbf{x})
\end{aligned}
\tag{14}
$$

where, $\mathbf{y}^I$ represents the source points located on the interface; c^{I} is the free term coefficient, and for smooth interface, the expression of c^I is

$$
c^I = \frac{1}{2}[k_1(\mathbf{y}^I) + k_2(\mathbf{y}^I)] \tag{15}
$$

where, $k_1(\mathbf{y}^I)$ and $k_2(\mathbf{y}^I)$ are the thermal conductivities for the adjacent two different materials on the location of $\mathbf{y}^I$.

For the convenience, taking into account Eqs. (9) and (10), we can rewrite Eqs. (13) and (14) in an uniform form

$$
\begin{aligned}
\hat{k}(\mathbf{y})\, T(\mathbf{y},t) = & -\int_\Gamma G(\mathbf{x},\mathbf{y})\, q(\mathbf{x},t)\, d\,\Gamma(\mathbf{x}) - \int_\Gamma \frac{\partial G(\mathbf{x},\mathbf{y})}{\partial n} k(\mathbf{x})\, T(\mathbf{x},t)\, d\,\Gamma(\mathbf{x}) \\
& + \int_{\Gamma_I} \frac{\partial G(\mathbf{x},\mathbf{y})}{\partial n'} \Delta k(\mathbf{x})\, T(\mathbf{x},t)\, d\,\Gamma(\mathbf{x}) + \int_\Omega G(\mathbf{x},\mathbf{y})\, Q(\mathbf{x})\, d\,\Omega(\mathbf{x}) \\
& + \int_{\overline{\Omega}} \hat{V}(\mathbf{x},\mathbf{y})\, T(\mathbf{x},t)\, d\,\Omega(\mathbf{x}) - \int_\Omega \rho(\mathbf{x}) c_p(\mathbf{x})\, G(\mathbf{x},\mathbf{y}) \frac{\partial T(\mathbf{x},t)}{\partial t}\, d\,\Omega(\mathbf{x})
\end{aligned}
\tag{16}
$$

where,

$$\hat{k}(\mathbf{y}) = \begin{cases} \frac{1}{2}k(\mathbf{y}) & \text{for smooth outer boundary points on } \Gamma \\ \frac{1}{2}[k_1(\mathbf{y}) + k_2(\mathbf{y})] & \text{for smooth interface points on } \Gamma_{\mathrm{I}} \\ k(\mathbf{y}) & \text{for internal points in } \overline{\Omega} \end{cases} \tag{17}$$

$$\hat{V}(\mathbf{x},\mathbf{y}) = \frac{\partial G(\mathbf{x},\mathbf{y})}{\partial x_i}\frac{\partial k(\mathbf{x})}{\partial x_i} \tag{18}$$

To avoid discretizing the domain Ω into internal cells for evaluating domain integrals involved in the above integral equations using the conventional cell-integration technique [39], a robust transformation technique from domain integrals into equivalent boundary integrals is described in reference [19]. In the paper, the three domain integrals involved in Eq.(16) are transformed into equivalent boundary integrals by the radial integration method (RIM) [13].

4. Numerical implementation

Eq. (16) is the boundary-interface-domain integral equation for solving multi-medium transient heat conduction problems with variable material properties, and by employing RIM transforming the involved domain integrals into equivalent boundary integrals, a pure boundary element method without internal cells can be developed.

4.1 System of differential equations

After discretizing the outer boundary Γ and interface Γ_I into a series of boundary elements and collocating the source point $\mathbf{y}$ through all boundary, interface, and internal nodes, we can form the system of differential equations for Eq.(16). Assuming that the BEM model involves N_b boundary nodes, N_c interface nodes, and N_i internal nodes, the total number of nodes is $N_A = N_b + N_c + N_i$. The discrete form of integral equation (16) is as follows:

$$\begin{bmatrix} \mathbf{H}_{bb} & \mathbf{H}_{bc} & \mathbf{0} \\ \mathbf{H}_{cb} & \mathbf{H}_{cc} & \mathbf{0} \\ \mathbf{H}_{ib} & \mathbf{H}_{ic} & \mathbf{H}_{ii} \end{bmatrix}_{N_A \times N_A} \begin{Bmatrix} \mathbf{T}_b \\ \mathbf{T}_c \\ \mathbf{T}_i \end{Bmatrix}_{N_A} = \begin{bmatrix} \mathbf{G}_{bb} \\ \mathbf{G}_{cb} \\ \mathbf{G}_{ib} \end{bmatrix}_{N_A \times N_b} \mathbf{q}_b + \begin{Bmatrix} \mathbf{f}_b \\ \mathbf{f}_c \\ \mathbf{f}_i \end{Bmatrix}_{N_A} + \mathbf{V}_{N_A \times N_A}\mathbf{T} - \mathbf{C}_{N_A \times N_A}\dot{\mathbf{T}}_A \tag{19}$$

where, $\mathbf{H}_{bc}$, $\mathbf{H}_{cc}$ and $\mathbf{H}_{ic}$ correspond to the coefficients of the interface integrals; $\mathbf{H}_{bb}$, $\mathbf{H}_{cb}$, $\mathbf{H}_{ib}$ and $\mathbf{G}_{bb}$, $\mathbf{G}_{cb}$ $\mathbf{G}_{ib}$ correspond to the outer boundary integrals; $\mathbf{H}_{ii}$ is diagonal matrix consisting of free term coefficients for internal points. $\mathbf{V}$ and $\mathbf{C}$ (both with dimensions of $N_A \times N_A$) correspond to the last two domain integrals in Eq.(16). And $\mathbf{f}_b$, $\mathbf{f}_c$

and $\mathbf{f}_i$ are the domain integration results for heat sources. $\mathbf{T}_b$ and $\mathbf{q}_b$ are the temperatures and heat fluxes for the boundary nodes respectively, and

$$\mathbf{T}_b = \begin{Bmatrix} \overline{\mathbf{T}}_1 \\ \mathbf{T}_2 \end{Bmatrix}, \quad \mathbf{q}_b = \begin{Bmatrix} \mathbf{q}_1 \\ \overline{\mathbf{q}}_2 \end{Bmatrix} \tag{20}$$

In which, $\overline{\mathbf{T}}_1$ and $\overline{\mathbf{q}}_2$ are the given temperatures on the Dirichlet boundaries and and heat fluxes on the Neumann boundaries, respectively.

Rearrange the system of equations Eq.(19) by transposing columns of [**H**], [**G**] and [**V**] from one side to the other, gathering all unknowns to the left-hand side, then we can rewrite Eq.(19) as

$$\mathbf{A}\,\mathbf{x} = \mathbf{y} - \mathbf{C}\,\dot{\mathbf{T}} \tag{21}$$

where,

$$\mathbf{x} = \begin{Bmatrix} \mathbf{q}_1 \\ \mathbf{T}_2 \\ \mathbf{T}_c \\ \mathbf{T}_i \end{Bmatrix} = \begin{Bmatrix} \mathbf{q}_1 \\ \mathbf{T}_x \end{Bmatrix} \tag{22}$$

In which, $\mathbf{T}_x$ consists of unknown temperatures on the Neumann boundary conditional nodes, the interface nodes and internal nodes.

By writing the coefficient matrices $\mathbf{A}$, $\mathbf{C}$ in block form, we can reconstitute Eq.(21) as follows:

$$\begin{bmatrix} \mathbf{A}_{11} & \mathbf{A}_{1x} \\ \mathbf{A}_{x1} & \mathbf{A}_{xx} \end{bmatrix} \begin{Bmatrix} \mathbf{q}_1 \\ \mathbf{T}_x \end{Bmatrix} = \begin{Bmatrix} \mathbf{y}_1 \\ \mathbf{y}_x \end{Bmatrix} - \begin{bmatrix} \mathbf{C}_{11} & \mathbf{C}_{1x} \\ \mathbf{C}_{x1} & \mathbf{C}_{xx} \end{bmatrix} \begin{Bmatrix} \dot{\mathbf{T}}_1 \\ \dot{\mathbf{T}}_x \end{Bmatrix} \tag{23}$$

In Eq.(21), the unknown heat fluxes at nodes on Dirichlet boundary can be expressed by the unknown temperatures as following

$$\mathbf{q}_1 = [\mathbf{A}_{11}]^{-1}(\mathbf{y}_1 - \mathbf{A}_{1x}\mathbf{T}_x - \mathbf{C}_{11}\dot{\mathbf{T}}_1 - \mathbf{C}_{1x}\dot{\mathbf{T}}_x) \tag{24}$$

Given that $\mathbf{T}_1$ are known temperatures on Dirichlet boundary, which do not vary with time, therefore $\dot{\mathbf{T}}_1 = \mathbf{0}$, substituting back into Eq.(24) yields the following equation:

$$\mathbf{q}_1 = \overline{\mathbf{E}}_{1x}\mathbf{T}_x + \overline{\mathbf{D}}_{1x}\dot{\mathbf{T}}_x + \overline{\mathbf{F}}_1 \tag{25}$$

where,

$$\overline{\mathbf{E}}_{1x} = -[\mathbf{A}_{11}]^{-1}\mathbf{A}_{1x} \tag{26}$$

$$\overline{\mathbf{D}}_{1x} = -[\mathbf{A}_{11}]^{-1}\mathbf{C}_{1x} \tag{27}$$

$$\overline{\mathbf{F}}_{1} = [\mathbf{A}_{11}]^{-1}\mathbf{y}_{1} \tag{28}$$

Substituting Eq.(25) back to Eq.(23), $\mathbf{q}_1$ can be eliminated from the system of differential equations, and the regularized form of differential equations that is only concerned with temperature can be derived:

$$\overline{\mathbf{A}}_{xx}\dot{\mathbf{T}}_{x} = \overline{\mathbf{B}}_{xx}\mathbf{T}_{x} + \overline{\mathbf{C}}_{xx}\dot{\mathbf{T}}_{1} + \overline{\mathbf{Y}}_{x} \tag{29}$$

Similarly, $\dot{\mathbf{T}}_1 = \mathbf{0}$ with the assumption that the temperature boundary conditions do not vary with time, Eq.(29) can be changed into the following form

$$\overline{\mathbf{A}}_{xx}\dot{\mathbf{T}}_{x} = \overline{\mathbf{B}}_{xx}\mathbf{T}_{x} + \overline{\mathbf{Y}}_{x} \tag{30}$$

where,

$$\overline{\mathbf{A}}_{xx} = \mathbf{C}_{xx} - \mathbf{A}_{x1}[\mathbf{A}_{11}]^{-1}\mathbf{C}_{1x} \tag{31}$$

$$\overline{\mathbf{B}}_{xx} = \mathbf{A}_{x1}[\mathbf{A}_{11}]^{-1}\mathbf{A}_{1x} - \mathbf{A}_{xx} \tag{32}$$

$$\overline{\mathbf{Y}}_{x} = \mathbf{y}_{x} - \mathbf{A}_{x1}[\mathbf{A}_{11}]^{-1}\mathbf{y}_{1} \tag{33}$$

Now, Eq.(30) is the normalized system of differential equations only concerned with unknown temperatures. To solve the time-dependent system of equations Eq. (30), the finite difference method (FDM) or precise integration method (PIM) [15] can be used to approximate the time evolution of temperatures. In this paper, we adopt the backward differentiation scheme [42], which is unconditionally stable and non-oscillatory in solving system of ordinary differential equations, to solve Eqs.(30) and (25).

4.2 Time marching scheme

To solve the equation set (30) and (25), we adopt the finite difference method to approximate the time derivative term:

$$\dot{\mathbf{T}}_{x} = \frac{\mathbf{T}_{x}^{n+1} - \mathbf{T}_{x}^{n}}{\Delta t} \tag{34}$$

$$\mathbf{T}_{x} = \theta\,\mathbf{T}_{x}^{n+1} + (1-\theta)\mathbf{T}_{x}^{n} \tag{35}$$

where, $\mathbf{T}_x^n$ represents the temperature at the *n*-th time step, and θ is the Euler parameter which usually takes a value between 0.5 and 1 [40]. In this study, we take $\theta = 1$. Substituting Eqs.(34) and (35) into Eq.(30), yields

$$\mathbf{T}_{x}^{n+1} = \mathbf{M}\mathbf{T}_{x}^{n} + \mathbf{N} \tag{36}$$

where,

$$\mathbf{M} = [\overline{\mathbf{A}}_{xx} / \Delta t - \theta\, \overline{\mathbf{B}}_{xx}]^{-1} [\overline{\mathbf{A}}_{xx} / \Delta t + (1-\theta) \overline{\mathbf{B}}_{xx}] \tag{37}$$

$$\mathbf{N} = [\overline{\mathbf{A}}_{xx} / \Delta t - \theta\, \overline{\mathbf{B}}_{xx}]^{-1} \overline{\mathbf{Y}}_{x} \tag{38}$$

where $\overline{\mathbf{A}}_{xx}$, $\overline{\mathbf{B}}_{xx}$ and $\overline{\mathbf{Y}}_{x}$ are defined by Eqs.(31)-(33).

With a similar process, substituting Eqs.(34) and (35) into Eq.(25), the heat fluxes $\mathbf{q}_1$ at nodes on Dirichlet boundary can be evaluated at each time step:

$$\mathbf{q}_1^{n+1} = \mathbf{J}\, \mathbf{T}_x^{n+1} + \mathbf{K}\, \mathbf{T}_x^{n} + \overline{\mathbf{F}}_1 \tag{39}$$

where,

$$\mathbf{J} = \theta\, \overline{\mathbf{E}}_{1x} + \overline{\mathbf{D}}_{1x} / \Delta t \tag{40}$$

$$\mathbf{K} = (1-\theta)\, \overline{\mathbf{E}}_{1x} - \overline{\mathbf{D}}_{1x} / \Delta t \tag{41}$$

In Eqs.(39)-(41), $\overline{\mathbf{E}}_{1x}$, $\overline{\mathbf{D}}_{1x}$ and $\overline{\mathbf{F}}_1$ are determined by Eqs.(26)-(28). Now, Eq.(36) and Eq.(39) can be employed to trace the time evolution of temperature and heat flux.

5. Numerical example

A Fortran code, named SIEBEM (single interface integral equation boundary element method) using the presented interface integral formulations in this paper has been developed.

5.1 Transient heat conduction in a two-media composed square flange

This example focuses on a square flange with four reinforced mounting holes, which are equally distributed along a circle with radius of $\Phi = 5.374\,\text{cm}$, as shown in Fig. 2. The flange and the mounting holes are made of different materials, marked with different colors in Fig.2. The initial temperature is assumed to be $T_0 = 0$℃. The temperature at the inner circular side suddenly changes to 800℃, while the temperature at the outer side of the square keeps 0℃. Inner sides of the mounting holes are temperature insulated.

Due to symmetry of the flange, only a quarter is analyzed. The geometry and boundary conditions are shown in Fig. 3, where point O(x=0, y=0) is the spatial origin, point C (x =3.8, y =3.8) represents the center of the mounting hole. Symbols Ω_1 and Ω_2 are the computational domains for two different media, respectively.

The material properties for media Ω_1 and Ω_2 are listed in Table 1, where k represents the thermal conductivity, c_p represents the specific heat, and ρ the mass density.

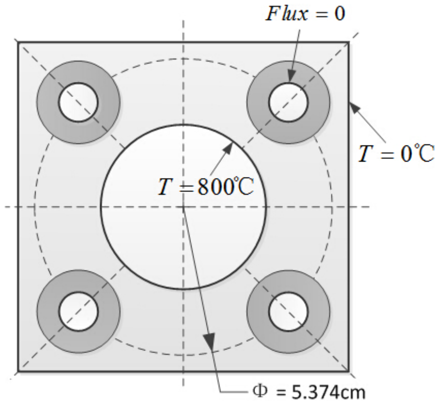

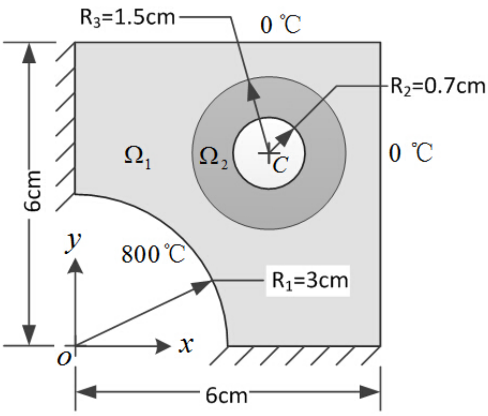

Figure 2. Square flange **Figure 3. Quarter of the flange**

Table 1. Material properties for each medium

Medium	k (W/m·K)	c_p (J/kg·K)	ρ (kg/m^3)
Ω_1	200	490	8.9×10^3
Ω_2	40	900	6.6×10^3

The inner circular side of the flange is discretized into 30 equally-spaced linear boundary elements, and each of the two straight outer boundary lines is discretized into 35 equally-spaced linear elements. The whole BEM model employs 998 nodes, in which 180 are outer boundary nodes, 40 are interface nodes, and 778 are internal nodes distributed within the domain. Fig. 4 shows the BEM model for computation. For comparison, this model is also analyzed using the conventional multi-domain boundary element method (MDBEM) reported in [25]. By using the same scale of mesh discretization, the MDBEM shown in Fig. 5 employs 998 nodes and 260 boundary elements. Since the interface marked with 'F' shown in Fig.5 has to be discretized into elements in each medium, the number of elements used in the MDBEM model is bigger than that used in the SIEBEM model. Therefore the computation scale for the MDBEM model is bigger than that of the SIEBEM model.

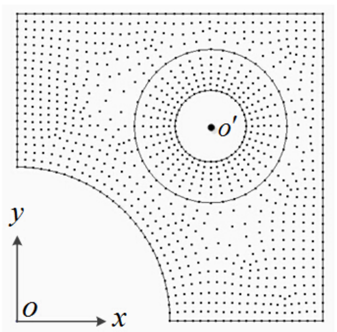

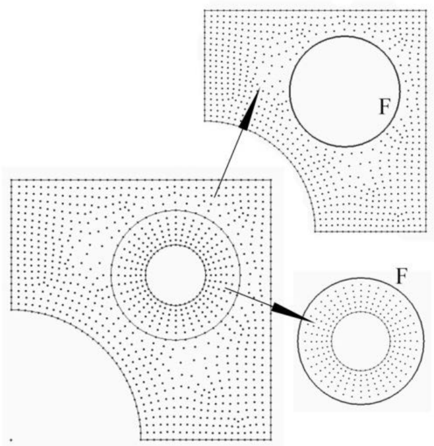

Figure 4. SIEBEM model **Figure 5. MDBEM model**

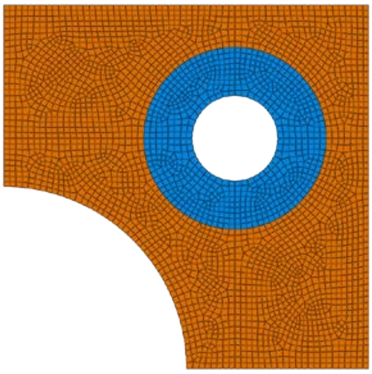

Figure 6. FEM mesh

A 10s time period is analyzed with 100 equally discretized time steps, and the length of each time step is $\Delta t = 0.1\,\text{s}$. To provide a reference solution to compare with the BEM results, the solution of this problem is computed using the commercial software ABAQUS. Fig.6 shows the FEM mesh.

Around the inner circle of the mounting hole with radius of R_2=0.7cm, the temperature distribution at different times calculated by SIBEM, MDBEM and FEM software are shown in Fig.7. And Fig.8 shows the temperature distribution along x direction at the y =0 symmetric straight edge. Fig. 9 compares the BEM results with FEM results for the temperature with time around the interface circle with the radius R_3=1.5cm in Fig.3. From Figs. 7 - 9, we can see that the results of SIEBEM coincide well with the results of MDBEM and FEM software, which validates the correctness of the presented method.

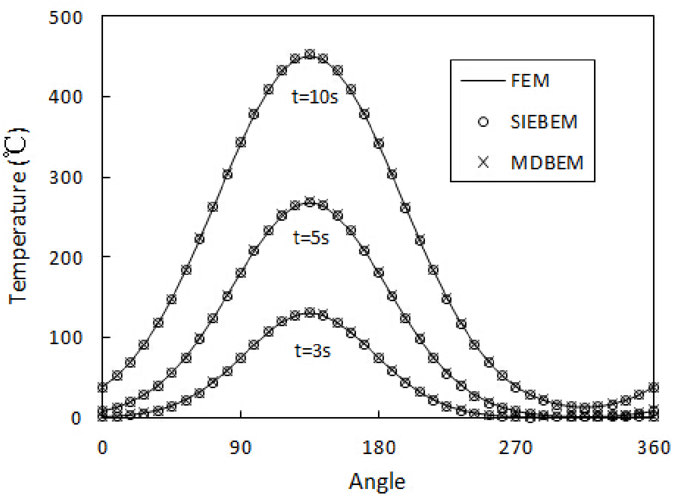

Figure 7. Temperature distribution along inner circle R2=0.7cm

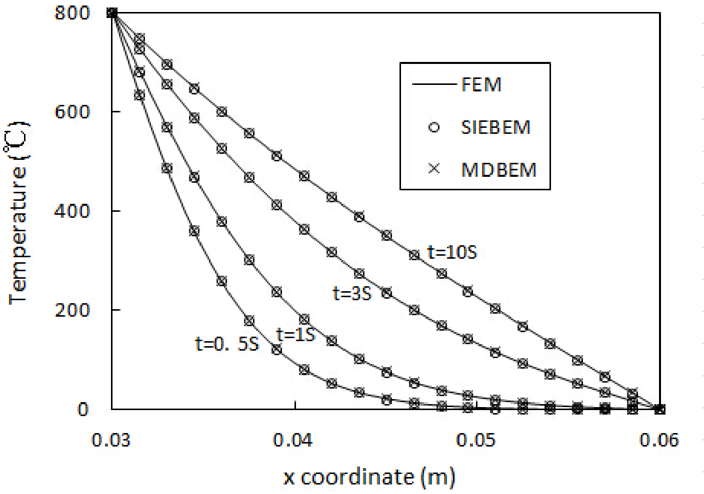

Figure 8. Temperature distribution along the y = 0 straight edge

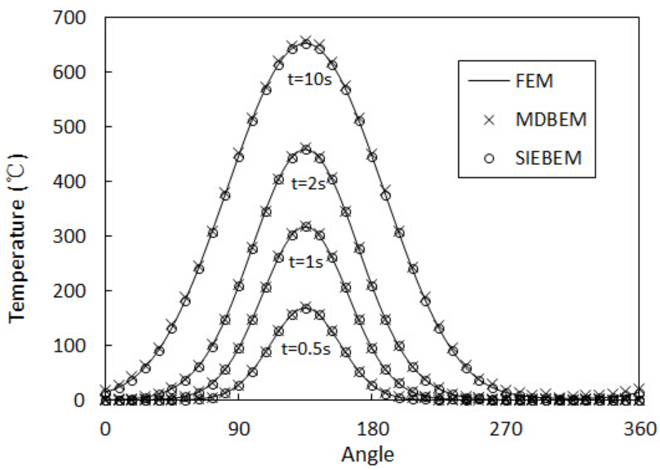

Figure 9. Temperature distribution along the interfacial circle R_3=1.5cm

Fig.10 shows the contour plots of the temperature distribution at different time. From Fig.10, we can easily find the discontinuous effect of temperature distribution when crossing the interfacial circle between the body of the flange and the mounting hole.

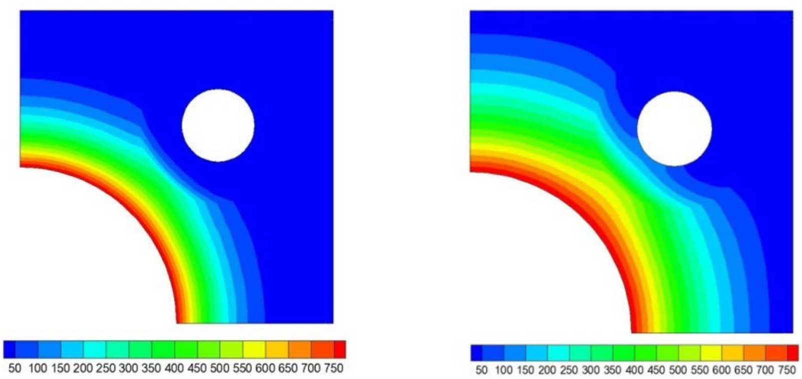

a ***b***

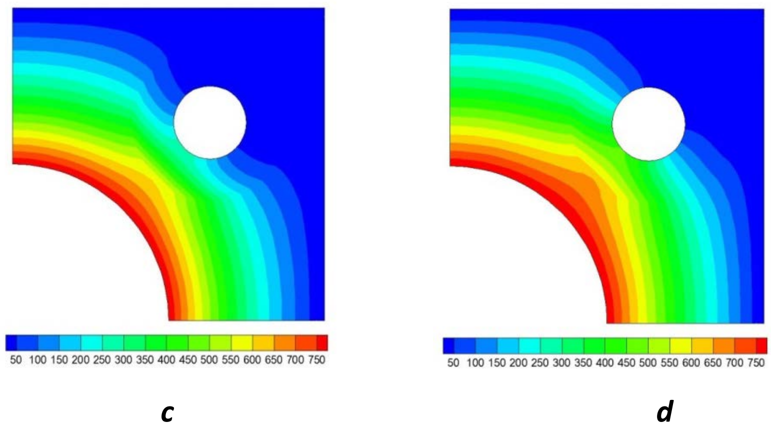

Figure 10. Counter plot of the temperature at different times:

(*a*) *t* = 1s ; (*b*) *t* = 2s; (*c*) *t* = 5s; (*d*) *t* = 10s

5.2 3D transient heat conduction in a four-media composed hollow cylinder

The third example to be considered is a hollow cylinder with a reinforcing stair, which is composed of four different media denoted by Ω_1, Ω_2, Ω_3 and Ω_4, as shown in Fig.11 (*a*) . The initial temperature is assumed to be T_0=0℃. Then the temperature at the top surface changes to 800℃, while the temperature at the bottom surface stays as 0℃. The other sides are thermally insulated. Due to symmetry of the problem, only a quarter of the hollow cylinder is modeled. Figs. 11(*b*) and 11(*c*) shows detailed dimensions and boundary conditions for the geometrical model.

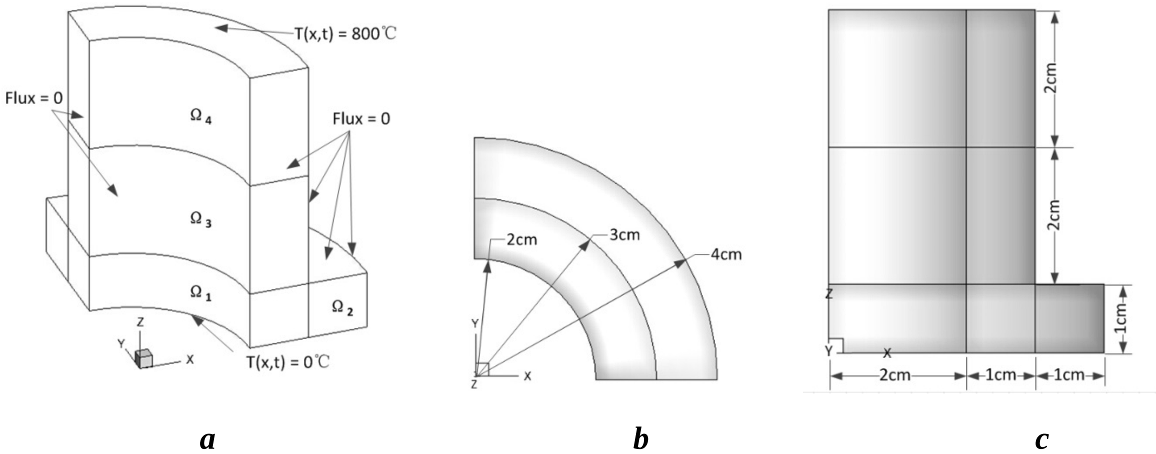

Figure 11. Four-media composed hollow cylinder: (*a*) 3D global view; (*b*) top view;

(*c*) right-side view

The material properties of the four media are prescribed as functions of spatial coordinates, and Table 2 gives these specific functions of coordinates for each medium. In order to show the variation of material properties with respect to the spatial coordinates more vividly, the profiles of thermal conductivity k and specific heat c_p are illustrated in Fig. 12. From Fig.12 we can see that the material properties vary in space continuously within each medium but jump across the interfaces between different media.

Table 2. Material properties for each medium

	k (W/m·K)	c_p (J/kg·K)	ρ (kg/m^3)
Ω_1	$200\times e^{50z}$	$500\times e^{30z}$	8900
Ω_2	$400+10^4(\sqrt{x^2+y^2}-0.03)$	$900-2\times10^4(\sqrt{x^2+y^2}-0.03)$	2700
Ω_3	$200+10^4(z - 0.01)$	$500-10^4(z-0.01)$	7900
Ω_4	$600-10^6(z-0.03)^2$	$700-5\times10^5(z-0.03)^2$	6900

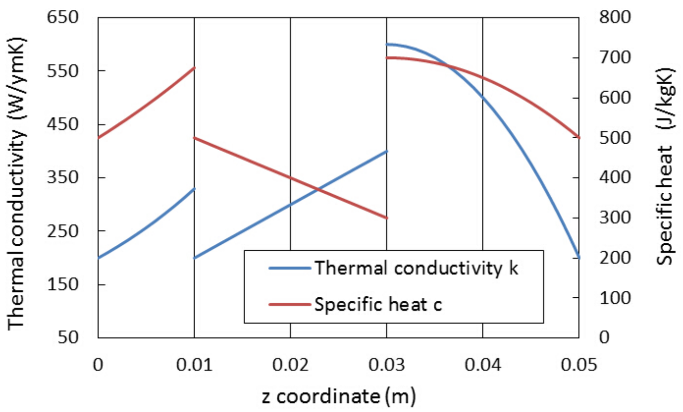

Figure 12. Profiles of thermal conductivity and specific heat along *z*-direction

The BEM mesh employs 880 4-node linear elements, in which 144 are interface elements distributed on the three interfaces between every two different media. Discontinuous elements are used at the intersection points between the interface and outer boundary, ensuring that a collocation point is either used by an outer boundary element or an interface element, see Fig. 13. The total number of nodes is 1546, among which 823 are boundary nodes, 195 are interface nodes, and 528 are internal nodes. Fig. 13 shows the BEM model for computation, in which different media are marked with different colors.

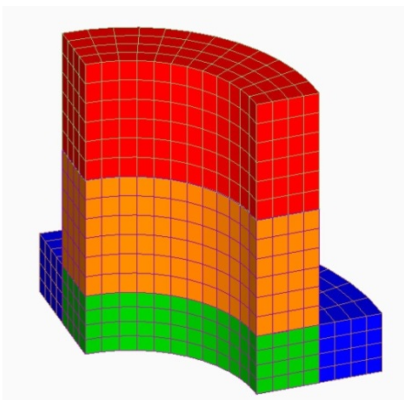

Figure 13. BEM mesh for the hollow cylinder

A 10 second time period is analyzed with 100 equally discretized time steps, and the length of each time step is Δt = 0.1s. For comparison, this model is also analyzed with ABAQUS by using the UMATHT subroutine [43]. Fig. 14 shows the distribution of temperature along z direction over the inner side vertical line of x = 2 cm and y = 0 cm. Fig. 15 shows the temperature distribution along x direction over the spatial straight line of y = 0 cm and z = 1 cm. From Figs. 14 and 15 we can see that the BEM results coincide well with the FEM results, demonstrating the correctness of the proposed method. From Fig. 14, we can easily find that three segment of curves compose the profile of temperature at each time step. And in Fig.15, the profile is composed by two segments. This effect is caused by the jump effect of material properties in multi-medium problems.

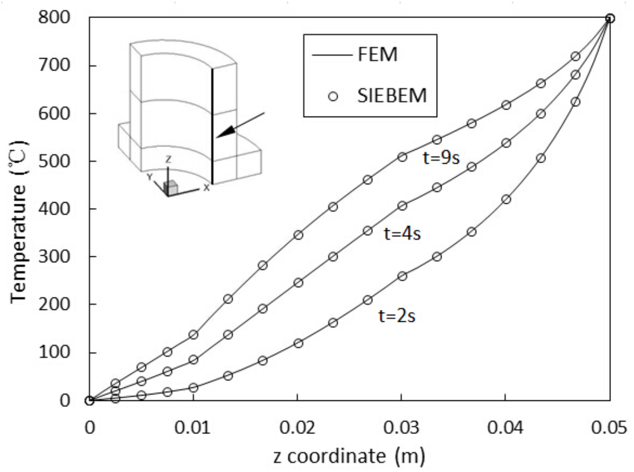

Figure 14.   Temperature distribution along the z coordinate direction

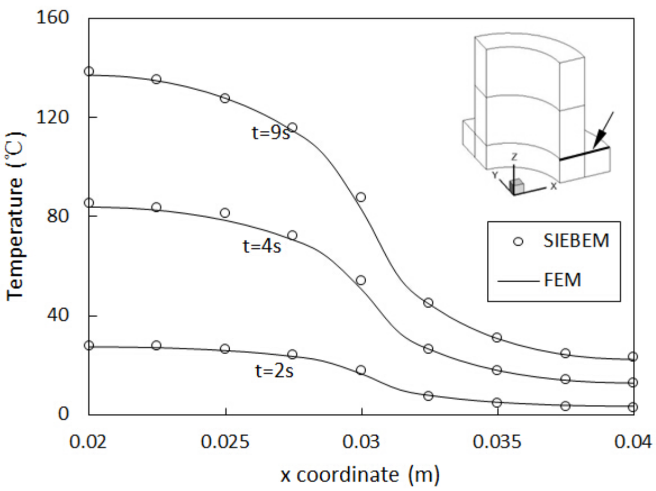

Figure 15.   Temperature distribution along the *x* coordinate direction

To examine the time evolution of temperature, three points A (1.7678, 1.7678, 3), B (1.4142, 1.4142, 4) and C (1.4142, 1.4142, 2), are investigated. Table 3 shows the comparison of the temperature results at each time step between BEM and FEM method. Relative errors are also calculated, taking the ABAQUS results as standard values. From Table 3 we can see that the relative errors converge to zero with time evolution, indicating that the presented method is stable with time.

Table 3. Computed temperatures at points *A*, *B* and *C* with Δt = 0.1s

	A			*B*			*C*		
t(s)	BEM	Abaqus	Error(%)	BEM	Abaqus	Error(%)	BEM	Abaqus	Error(%)
1	125.116	123.891	0.989	292.614	290.528	0.718	35.345	35.523	-0.500
2	262.106	260.178	0.741	421.561	419.452	0.503	121.269	120.420	0.705
3	350.276	348.363	0.549	493.677	491.700	0.402	194.533	193.266	0.656
4	408.304	406.638	0.410	539.235	537.480	0.326	247.504	246.302	0.488
5	447.202	445.886	0.295	569.295	567.807	0.262	284.317	283.406	0.321
6	473.492	472.552	0.199	589.482	588.271	0.206	309.561	309.012	0.178
7	491.323	490.739	0.119	603.138	602.187	0.158	326.784	326.588	0.060
8	503.434	503.161	0.054	612.403	611.681	0.118	338.511	338.627	-0.034
9	511.665	511.653	0.002	618.696	618.167	0.086	346.688	346.865	-0.051
10	517.470	517.458	0.002	622.974	622.601	0.060	352.483	352.500	-0.005

To examine the influence of the length of each time step Δt on the computed results, temperatures at points *A*, *B* and *C* are also computed by using different values of Δt. Fig. 16 (*a*) shows the change of relative errors using the time step Δt = 2s. In Fig.16 (*a*), both SIEBEM and ABAQUS results are calculated on Δt = 2s, and the ABAQUS results are utilized as the standard values. Meantime, Fig. 16 (*b*) shows the change of relative errors using Δt = 0.04s, equally the ABAQUS results on Δt = 0.04s are also given as the standard values. By comparing Figs. 16 (*a*) and 16 (*b*) we can see that, even Δt = 2s is 50 times the length of Δt = 0.04s, the results calculated by SIEBEM coincide well with ABAQUS results, and their relative errors converge to zero, indicating that the presented method is stable and highly precise.

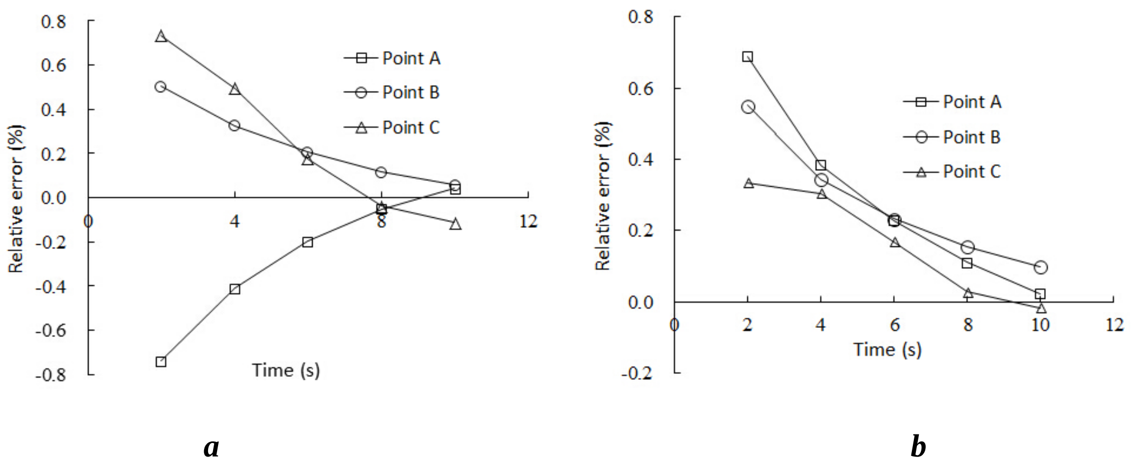

Figure 16. Relative errors of temperature along with time: (*a*) Δt = 2s; (*b*) Δt = 0.04s

6. Conclusions

In this paper, based on a newly derived interface integral equation, a new and simple BEM characterized as interface integral equation method is developed for solving transient heat conduction in multi-medium materials with variable material properties. To solve the time-dependent system of differential equations, firstly the unknown heat fluxes are eliminated from the system of differential equations, then based on an implicit backward differentiation scheme, an unconditionally stable and non-oscillatory time marching solution scheme is developed for solving the normal time-dependent system of equations.

Acknowledgement

The authors gratefully acknowledge the National Natural Science Foundation of China (11172055, 11202045).

References

[1] Wrobel, L. C. and Brebbia, C. A. (1992) *Boundary Element Methods in Heat Transfer*, Computational Mechanics Publications, Boston.

[2] Divo, E. and Kassab, A. J. (2003) *Boundary Element Method For Heat Conduction: With Applications in Non-Homogeneous Media*, WIT Press, Southampton, UK.

[3] Gao, X. W., Peng, H. F., Yang, K. and Wang, J. (2015) *Higher Boundary Element Method - Theory and Programming* (Chinese edition), Science Press, Beijing, 2015. ISBN: 978-7-03-042689-5

[4] Liu, Y. J., Mukherjee, S., Nishimura, N., Schanz, M., Ye, W., Sutradhar, A., Pan, E., Dumont, N. A., Frangi, A. and Saez, A. (2011) Recent advances and emerging applications of the boundary element method, *ASME Applied Mechanics Reviews* **64**, 617-636.

[5] Rizzo, F. J. and Shippy, D. J. (1970) A method of solution for certain problems of transient heat conduction, *AIAA Journal* **8**, 2004-2009.

[6] Sutradhar, A., Paulino, G. H. and Gray, L. J. (2002) Transient heat conduction in homogeneous and non-homogeneous materials by the Laplace transform Galerkin boundary element method, *Engineering Analysis with Boundary Elements* **26**, 119-132.

[7] Sutradhar, A., and Paulino, G. H. (2004) The simple boundary element method for transient heat conduction in functionally graded materials, *Computer Methods in Applied Mechanics and Engineering* **193**, 4511-4539.

[8] Simoes, N., Tadeu, A., Antonio, J. and Mansur, W. (2012) Transient heat conduction under nonzero initial conditions: A solution using the boundary element method in the frequency domain, *Engineering Analysis with Boundary Elements* **36**, 562-567.

[9] Guo, S. P., Zhang, J. M., Li, G. Y. and Zhou, F. L. (2013) Three-dimensional transient heat conduction analysis by Laplace transformation and multiple reciprocity boundary face method, *Engineering Analysis with Boundary Elements* **37**, 15-22.

[10] Wrobel, L. C. and Brebbia, C. A. (1981) A formulation of the boundary element method for axisymmetric transient heat conduction, *International Journal of Heat and Mass Transfer* **24**, 843-850.

[11] Ochiai, Y., Sladek, V. and Sladek, J. (2006) Transient heat conduction analysis by triple-reciprocity boundary element method, *Engineering Analysis with Boundary Elements* **30**, 194-204.

[12] Tanaka, M., Matsumoto, T. and Takakuwa, S. (2006) Dual reciprocity BEM for time-stepping approach to the transient heat conduction problem in nonlinear materials, *Computer Methods in Applied Mechanics and Engineering* **195**, 4953-4961.

[13] Yang, K. and Gao, X. W. (2010) Radial integration BEM for transient heat conduction problems, *Engineering Analysis with Boundary Elements* **34**, 557-563.

[14] Al-Jawary, M. A., Ravnik, J., Wrobel, L. C. and Skerget, L. (2012) Boundary element formulations for the numerical solution of two-dimensional diffusion problems with variable coefficients, *Computers and Mathematics with Applications* **64**, 2695-2711.

[15] Yu, B., Yao, W. A. and Gao, Q. (2014) A precise integration boundary-element method for solving transient heat conduction problems with variable thermal conductivity, *Numerical Heat Transfer Part B: Fundamentals* **45**, 472-493.

[16] Nardinia, D. and Brebbia, C. A., A new approach to free vibration analysis using boundary elements, *Applied Mathematical Modelling* **7,** 157-162.

[17] Partridge, P. W., Brebbia, C. A. and Wrobel, L. C. (1992) *The Dual Reciprocity Boundary Element Method*, Computational Mechanics Publications, Boston.

[18] Nowak, A. J. and Brebbia, C. A. (1989) The multiple-reciprocity method – a new approach for transforming BEM domain integrals to the boundary, *Engineering Analysis with Boundary Elements* **6**, 164-167.
[19] Gao, X. W. (2002) The radial integration method for evaluation of domain integrals with boundary-only discretization, *Engineering Analysis with Boundary Elements* **26**, 905-916.
[20] Divo, E. and Kassab, A. J. (1997) A generalized boundary-element method for steady-state heat conduction in heterogeneous anisotropic media, *Numerical Heat Transfer Part B-Fundamentals* **32**, 37-61.
[21] Kassab, A. J. and Divo, E. (1996) A generalized boundary integral equation for isotropic heat conduction with spatially varying thermal conductivity, *Engineering Analysis with Boundary Elements* **18**, 273-286.
[22] Divo, E. and Kassab, A. J. (1998) Generalized boundary integral equation for transient heat conduction in heterogeneous media, *Journal of Thermophysics and Heat Transfer* **12**, 364-373.
[23] Sladek, J., Sladek, V., Krivacek, J. and Zhang, Ch. (2003) Local BIEM for transient heat conduction analysis in 3-D axisymmetric functionally graded solids, *Computational Mechanics* **32**, 169-176.
[24] Sladek, J., Sladek, V. and Zhang, Ch. (2003) Transient heat conduction analysis in functionally graded materials by the meshless local boundary integral equation method, *Computational Materials Science* **28**, 494-504.
[25] Gao, X. W., Guo, L. and Zhang, Ch. (2007) Three-step multi-domain BEM solver for nonhomogeneous material problems, *Engineering Analysis with Boundary Elements* **31**, 965-973.
[26] Dong, C. Y. and de Pater, C. J. (2000) A boundary-domain integral equation for a coated plane problem, *Mechanics Research Communications* **27**, 643-652.
[27] Wang, C. B., Chatterjee, J. and P.K. Banerjee (2007) An efficient implementation of BEM for two- and three-dimensional multi-region elastoplastic analyses, *Computer Methods in Applied Mechanics and Engineering* **196**, 829-842.
[28] Zhou, A., Hui, K. and Lai, Y. (2008) Simulating deformation of objects with multi-materials using boundary element method, *International Journal for Numerical Methods in Engineering* **74**, 1088-1108.
[29] Giannopoulos, G. I. and Anifantis, N. K. (2007) A BEM analysis for thermomechanical closure of interfacial cracks incorporating friction and thermal resistance, *Computer Methods in Applied Mechanics and Engineering* **196**, 1018-1029.
[30] Divo, E., Kassab, A. J. and Rodriguez, F. (2003) Parallel domain decomposition approach for large-scale three-dimensional boundary-element models in linear and nonlinear heat conduction, *Numerical Heat Transfer Part B-Fundamentals* **44**, 417-437.
[31] Erhart, K., Divo, E. and Kassab, A. J. (2006) A parallel domain decomposition boundary element method approach for the solution of large-scale transient heat conduction problems, *Engineering Analysis with Boundary Elements* **30**, 553-563.
[32] Peng, H. F., Bai, Y. G., Yang, K. and Gao, X. W. (2013) Three-step multi-domain BEM for solving transient multi-media heat conduction problems, *Engineering Analysis with Boundary Elements* **37**, 1545-1555.
[33] Tanaka, M., T. Matsumoto and Takakuwa, S. (2006) Dual reciprocity BEM for time-steeping approach to the transient heat conduction problem in nonlinear materials, *Computer Methods in Applied Mechanics and Engineering* **195**, 4953-4961.
[34] Gao, X. W. and Wang, J. (2009) Interface integral BEM for solving multi-medium heat conduction problems, *Engineering analysis with boundary elements* **33**, 539-546.
[35] Gao, X. W. and Yang, K. (2009) Interface integral BEM for solving multi-medium elasticity problems, *Computer Methods in Applied Mechanics and Engineering* **198**, 1429-1436.
[36] Yang, K., Feng, W. Z. and Gao, X. W. (2015) A new approach for computing hyper-singular interface stresses in IIBEM for solving multi-medium elasticity problems, *Computer Methods in Applied Mechanics and Engineering* **287**, 54-68.
[37] Feng, W. Z., Gao, X. W., Liu, J. and Yang, K. (2015) A new BEM for solving 2D and 3D elastoplastic problems without initial stresses/strains, *Engineering Analysis with Boundary Elements* **61**, 134-144.
[38] Gao, X. W. (2006) A meshless BEM for isotropic heat conduction problems with heat generation and spatially varying conductivity, *International Journal for Numerical Methods in Engineering* **66**, 1411-1431.
[39] Gao, X. W. and Davies, T. G. (2002) *Boundary Element Programming in Mechanics*, Cambridge University Press, Cambridge, UK.
[40] Cui, M., Duan, W. W. and Gao, X. W. (2015) A new inverse analysis method based on a relaxation factor optimization technique for solving transient nonlinear inverse heat conduction problems, *International Journal of Heat and Mass Transfer* **90,** 491-498.
[41] Wang, H. T. and Yao, Z. H. (2013) Large-scale thermal analysis of fiber composites using a line-inclusion model by the fast boundary element method, *Engineering Analysis with Boundary Elements* **37,** 319-326.
[42] Zienkiewicz, O. C. and Taylor, K. L. (2000) *The Finite Element Method*, 5th edn . Butterworth Heinemann.
[43] ABAQUS Version 6.13 (2013) *Abaqus Analysis User's Guide,* Dassault System Simulia Corp., Providence, RI, USA.